Prepared for submission to JHEP DESY 14-250

Effects of subleading color in a parton shower

Zoltán Nagy[a] **and Davison E. Soper**[b]

[a] *DESY*
Notkestrasse 85
22607 Hamburg, Germany
[b] *Institute of Theoretical Science*
University of Oregon
Eugene, OR 97403-5203, USA

E-mail: Zoltan.Nagy@desy.de, soper@uoregon.edu

Abstract: Parton shower Monte Carlo event generators in which the shower evolves from hard splittings to soft splittings generally use the leading color (LC) approximation, which is the leading term in an expansion in powers of $1/N_c^2$, where $N_c = 3$ is the number of colors. In the parton shower event generator Deductor, we have introduced a more general approximation, the LC+ approximation, that includes some of the color suppressed contributions. In this paper, we explore the differences in results between the LC approximation and the LC+ approximation. Numerical comparisons suggest that, for simple observables, the LC approximation is quite accurate. We also find evidence that for gap-between-jets cross sections neither the LC approximation nor the LC+ approximation is adequate.

Keywords: perturbative QCD, parton shower

Contents

1 Introduction

Parton shower Monte Carlo event generators like Pythia [1], Herwig [2], and Sherpa [3] represent the momenta and flavors carried by partons in a natural way. One can imagine that at any "shower time" t in the development of the shower, there is a probability $\rho(t, \{p_\mathrm{a}, f_\mathrm{a}, p_\mathrm{b}, f_\mathrm{b}, p_1, f_1, \ldots, p_m, f_m\})$ to have m final state partons plus two initial state partons with the specified momenta p_l and flavors f_l. What happens between time t and $t + \Delta t$ is a change $\Delta\big|\rho(t)\big)$ chosen at random according to physics based parton splitting probabilities. The evolution of $\big|\rho(t)\big)$ is straightforwardly described in the language of classical statistical mechanics.

Spin and color do not fit easily into the event generator format because quantum interference between different spin and color states is important. For this reason, the natural language is that of quantum statistical mechanics. Then $\big|\rho(t)\big)$ represents not just a probability distribution, but a density matrix in color and spin space.

There is a fairly straightforward formalism [4] available to specify an evolution equation for $\big|\rho(t)\big)$ that takes full account of color and spin. Unfortunately, we do not know how to implement the full evolution equation in a practical computer program that would

constitute a parton shower event generator. If we use the leading color (LC) approximation and average over spins, we do get something practical [5].

We have implemented the resulting shower evolution equation as a parton shower event generator, DEDUCTOR [6, 7]. In ref. [6], we presented results from DEDUCTOR using the leading color approximation. However, there is an improved version of the leading color approximation that is still practical: the LC+ approximation [8]. The LC+ approximation is built into DEDUCTOR.

In this paper, we use the LC+ approximation to explore numerically the effect of color in a parton shower. We do not have a shower treatment with full color. It should be possible [8] to expand cross sections perturbatively in the difference between full color splitting functions and their LC+ approximations, but this possibility is not implemented in DEDUCTOR. Thus we are limited to looking at what we can discover with the LC+ approximation. From this investigation, two tentative conclusions emerge.

First, comparing results for simple observables calculated with the LC and LC+ approximations, we find differences of order $1/N_c^2 \approx 10\%$, but not larger differences. This is perhaps not a surprise, but real calculations were needed to reach this conclusion.

Second, in events with two high p_T jets with a large rapidity separation between them, we find that there is a substantial influence of color on the probability to have a gap between the two jets that contains no jets with transverse momentum above a cut p_T^{cut}. Here, neither the LC approximation nor the LC+ approximation is adequate.

This paper is organized as follows. We provide some background information in section 2. Then in section 3 we investigate how much color suppression is typical in the color state as the shower develops. (The brief answer is that it is rare to have no color suppression.) In sections 4 and 5, we look at the difference between LC results and LC+ results for two simple observables: the one jet inclusive cross section and the distribution of the number of partons in a jet (which is not really physically observable, but is calculable with a fixed cutoff on the k_T in parton splittings). In sections 6 and 7, we examine the influence of color on the cross section to have a gap between high p_T jets. We present some conclusions in section 8. There is an appendix about how to switch from the LC+ approximation to the LC approximation part way into the shower.

2 Background

Before exploring numerical results, we provide a little background about DEDUCTOR and about color and the LC+ approximation.

2.1 Deductor

A brief presentation of the parton shower event generator DEDUCTOR can be found in ref. [6]. Here, we simply mention some major features. First, DEDUCTOR generates a parton shower, but does not at present include a hadronization stage. Nor does it include an underlying event. Thus it is well suited as a tool for investigating the approximations in parton shower algorithms, but has some limitations for other uses. Second, DEDUCTOR averages over parton spins at each stage of splittings, in the same fashion as other parton

shower event generators. There is a method for including spin that should be practical [9], but we have not yet implemented it. Third, we argue in ref. [10] that it is best to order splittings in a parton shower in order of decreasing values of the virtuality in the splitting divided by the energy of the mother parton. This rather non-standard choice is implemented in DEDUCTOR. Fourth, initial state charm and bottom quarks have their proper masses in DEDUCTOR [11].

2.2 The color density matrix

The natural language for describing an evolving probability distribution in a parton shower is statistical mechanics. In order to include quantum color, we need *quantum* statistical mechanics. Thus we need a density operator that depends on the shower time t and is an operator on the space of color states of a possibly large number of partons. The density operator has the form

$$\rho(\{p,f\}_m,t) = \sum_{\{c\}_m,\{c'\}_m} \rho(\{p,f,c',c\}_m,t)\,\big|\{c\}_m\big\rangle\big\langle\{c'\}_m\big| \ . \tag{2.1}$$

Here $\big|\{c\}_m\big\rangle$ and $\big|\{c'\}_m\big\rangle$ are standard [12] basis vectors for the quantum color space for m final state partons plus two initial state partons [4, 8]. The color configuration $\{c\}_m$ of the ket state is, in general, different from the color configuration $\{c'\}_m$ of the bra state. Thus the function $\rho(\{p,f,c',c\}_m,t)$ depends on two sets of color indices. The density operator $\rho(\{p,f\}_m,t)$ can be regarded as a vector in the space of functions of $\{p,f\}_m$ with values in the space of operators on the quantum color space.

The color basis states are normalized to $\big\langle\{c\}_m\big|\{c\}_m\big\rangle = 1$ or to $\big\langle\{c\}_m\big|\{c\}_m\big\rangle \approx 1$ with very small corrections. They are not, however, generally orthogonal. However, when $\{c\}_m$ and $\{c'\}_m$ are different, one finds that $\big\langle\{c'\}_m\big|\{c\}_m\big\rangle = \mathcal{O}(1/N_{\rm c}^P)$ with $P \geq 1$. That is, the basis vectors are orthogonal in the $N_{\rm c} \to \infty$ limit.

At the end of a parton shower, one will want to measure something about the final state, using a color singlet measurement operator.[1] This means that we take the trace of $\rho(\{p,f\}_m,t)$ in the color space, so that the contribution from color states $\{c',c\}_m$ is proportional to $\big\langle\{c'\}_m\big|\{c\}_m\big\rangle$. That is, the contribution from color states with $\{c'\}_m \neq \{c\}_m$ is suppressed by one or more factors of $1/N_{\rm c}$.

One notes, however, that states with $\{c'\}_m \neq \{c\}_m$ are a natural part of quantum chromodynamics (QCD). They appear even at the Born level of a hard scattering, where we normally keep track of them by using color ordered amplitudes. Even if we start with $\{c'\}_m = \{c\}_m$ states, splittings in a parton shower generate $\{c'\}_m \neq \{c\}_m$ states.

2.3 The color suppression index

In order to understand the systematics how many factors of $1/N_{\rm c}$ accompany states with $\{c'\}_m \neq \{c\}_m$, it is useful to use the color suppression index [8].

[1] This leaves out hadronization. If we apply a hadronization model based on the formation of color strings, we do, in effect, apply a non-color-singlet measurement operator. We formulate how this can work in ref. [8].

To do that, we first note a small technical complication. In a $g \to q + \bar{q}$ splitting we have a color matrix $t^a_{ij} t^a_{i'j'}$ in the color amplitude. We can use the Fierz identity,

$$t^a_{ij} t^a_{i'j'} = \frac{1}{2}\,\delta_{ij'}\delta_{i'j} - \frac{1}{2N_\mathrm{c}}\,\delta_{ij}\delta_{i'j'}\ , \tag{2.2}$$

to write the result expanded in color basis states. At each $g \to q + \bar{q}$ splitting, shower evolution picks either the first, leading color, term or else the second, color suppressed, term. If the second term is chosen, further evolution uses the second color state, $\delta_{ij}\delta_{i'j'}$, and incorporates the factor $-1/(2N_\mathrm{c})$ into the weight factor for the event. We let p_E represent the number of times during the shower evolution that we pick up a $1/N_\mathrm{c}$ factor by using the second term in the Fierz identity.

With that complication out of the way, we can define the color suppression power P as the number of powers of $1/N_\mathrm{c}$ that appear at some stage of the shower coming from both the overlap $\big\langle \{c'\}_m \big| \{c\}_m \big\rangle$ of the color states, and the explicit $1/N_\mathrm{c}$ factors from $g \to q + \bar{q}$ splittings:

$$\left(\frac{1}{N_\mathrm{c}}\right)^{p_\mathrm{E}} \big\langle \{c'\}_m \big| \{c\}_m \big\rangle = \frac{c_P(m)}{N_\mathrm{c}^{P(m)}} \left\{ 1 + \mathcal{O}\left(\frac{1}{N_\mathrm{c}}\right) \right\}\ . \tag{2.3}$$

Now we define the color suppression index I. We simply use the group $U(N_\mathrm{c})$ in place of the true color group $SU(N_\mathrm{c})$ to calculate the color overlap

$$\left(\frac{1}{N_\mathrm{c}}\right)^{p_\mathrm{E}} \big\langle \{c'\}_m \big| \{c\}_m \big\rangle_{U(N_\mathrm{c})} = \frac{c_I(m)}{N_\mathrm{c}^{I(m)}} \left\{ 1 + \mathcal{O}\left(\frac{1}{N_\mathrm{c}}\right) \right\}\ . \tag{2.4}$$

The color suppression index has two properties that make it quite useful. First, we always have

$$P(m) \geq I(m)\ . \tag{2.5}$$

That is, if we use $I(m)$ to estimate the amount of color suppression, we can never overestimate. Second, at each stage of the shower, the color suppression index either stays the same or else it increases:

$$I(m+1) \geq I(m)\ . \tag{2.6}$$

Thus we can think of I as measuring color disorder, like entropy: it can never decrease as the shower evolves.

2.4 The LC and LC+ approximations

We have noted above that the hard scattering that leads to a parton shower has some contributions with $\{c'\}_m = \{c\}_m$ and thus with color suppression index $I = 0$.[2] It also generally has some contributions with $\{c'\}_m \neq \{c\}_m$ and thus with color suppression index $I > 0$. This implies that the associated probability has at least I powers of $1/N_\mathrm{c}$. As the shower develops, each parton splitting gives some terms that leave I unchanged, but also some terms that increase I. Thus, inevitably, we generate some color configurations that come with high powers of $1/N_\mathrm{c}$ and thus low probabilities.

[2] If the hard scattering is $2 \to 2$ parton-parton scattering, then $m = 2$ at the start of the parton shower.

The contributions with $I > 0$ are also associated with calculational difficulties in a parton shower. For this reason, it is common to start at the hard scattering with $\{c'\}_m = \{c\}_m$, $I = 0$ states only and then to omit generating any $I > 0$ states. In practice, it is very easy to avoid increasing I in parton splittings. In simplest terms, we count each gluon as carrying color $\mathbf{3} \times \bar{\mathbf{3}}$ instead of color $\mathbf{8}$. This gives us the leading color approximation.

We can also use the LC+ approximation [8]. Here we can start with $\{c'\}_m \neq \{c\}_m$, $I > 0$ states from the hard process. Then we can keep some of the terms with increasing I that are generated by parton splittings. We do not keep all of the terms, so this is still an approximation. The approximation is exact for collinear splittings and it is exact for splittings that are simultaneously collinear and soft. It does not, however, keep everything that arises from wide angle soft splittings. We refer the reader to ref. [8] for a full description.

With the LC+ approximation, we can eventually generate states with quite high values of the color suppression index I. Because these states come along with numerical weights, this has the effect of slowing down the numerical convergence of the program. That is, it takes more events to give the same statistical error. For this reason, we set a maximum value $(\Delta I)_{\max}$ for how much can be added to the color suppression index by the parton shower. When the amount of color suppression added by the shower, ΔI, reaches $(\Delta I)_{\max}$, we switch off the LC+ approximation and start using a version of the LC approximation that is adapted to $\{c'\}_m \neq \{c\}_m$. We describe how to do this in appendix A. For numerical results in this paper, we set $(\Delta I)_{\max} = 4$. Shower splitting either leaves I unchanged or increases it by two. Thus we are omitting terms with $\Delta I = 6$, corresponding to omitted factors as large as $1/N_c^6 \approx 10^{-3}$, which should allow for sufficient accuracy for any practical purpose. Of course, $(\Delta I)_{\max}$ is adjustable, so that we have an approximation with errors that can be controlled.

3 How much color suppression is typical?

Is it rare to generate a state with non-zero color suppression index I? To find out, we use DEDUCTOR to generate the cross section to make jets in proton-proton collisions at $\sqrt{s} = 14$ TeV. We select events that have a jet with $p_{\mathrm{T}} > 500$ GeV in the rapidity range $-2 < y < 2$. The parton shower generates splittings that are softer and softer, as measured by the virtuality parameter Λ^2 defined in ref. [10]. We stop the shower by not allowing any splittings with a splitting transverse momentum smaller than $k_{\mathrm{T}}^{\min} = 1$ GeV. This allows for quite a number of splittings: most of the cross section comes from events with twenty to fifty splittings. We show the distribution of the number of splittings in figure 1.

The hard process here is parton-parton scattering. We keep all of the contributions to the color-ordered amplitudes for parton-parton scattering. This gives an initial color density matrix of the form (2.1) with $m = 2$ for the two final state partons. We calculate the color suppression index I_2 just after the hard scattering according to eq. (2.4) with $p_{\mathrm{E}} = 0$. We find that, including the cases with $\{c'\}_2 \neq \{c\}_2$, the color suppression index can be $I_2 = 0$, 1, or 2. Now the shower starts. With each splitting, I has a chance to increase, so that $I_m \geq I_2$. We set a limit $I_m - I_2 \leq (\Delta I)_{\max}$ with $(\Delta I)_{\max} = 4$. If $I_m - I_2$

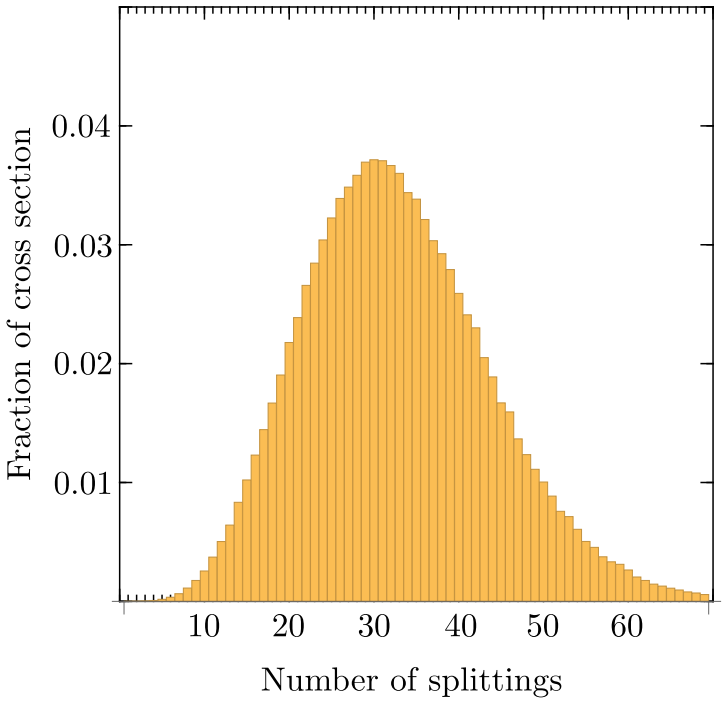

Figure 1. Probability of generating N splittings versus N in events that have a jet with $p_T > 500$ GeV in the rapidity range $-2 < y < 2$. The splitting cutoff is $k_T^{\min} = 1$ GeV.

reaches $I_{\max}$, we switch off the LC+ approximation and start using the extended version of the LC approximation that allows for $\{c'\}_m \neq \{c\}_m$.

We can answer the question of how rare it is to generate a non-zero color suppression index by plotting the fraction of the jet cross section coming from events that have a given value I_{N+2} after N splittings. We group $I_{N+2} = 1$ with $I_{N+2} = 2$, $I_{N+2} = 3$ with $I_{N+2} = 4$, and $I_{N+2} = 5$ with $I_{N+2} = 6$ because odd values of I (which are generated at the hard scattering) are rather rare. We plot the fraction of events with given values of I_{N+2} for N up to 50. For events with S splittings with $S < 50$, we define $I_{N+2} = I_{S+2}$ for $N > S$. We show a plot of the fraction of events with given values of I_{N+2} after N splittings in figure 2.

We can draw two lessons from figure 2. First, a little less than 10% of the cross section is associated with events that start with $I > 0$ right at the hard scattering. This is about what one would expect, since $1/N_c^2 \approx 0.1$. Second, it is rather rare for the partons to stay in an $I = 0$ state after many splittings. Only about 20% of the cross section comes from parton configurations that have $I = 0$ at the end of the shower. In fact, more than half of the cross section has $I > 2$ at the end of the shower. We would see more cross section associated with $I > 4$ at the end of the shower if we had not imposed $I_m - I_2 \leq 4$ on the shower.

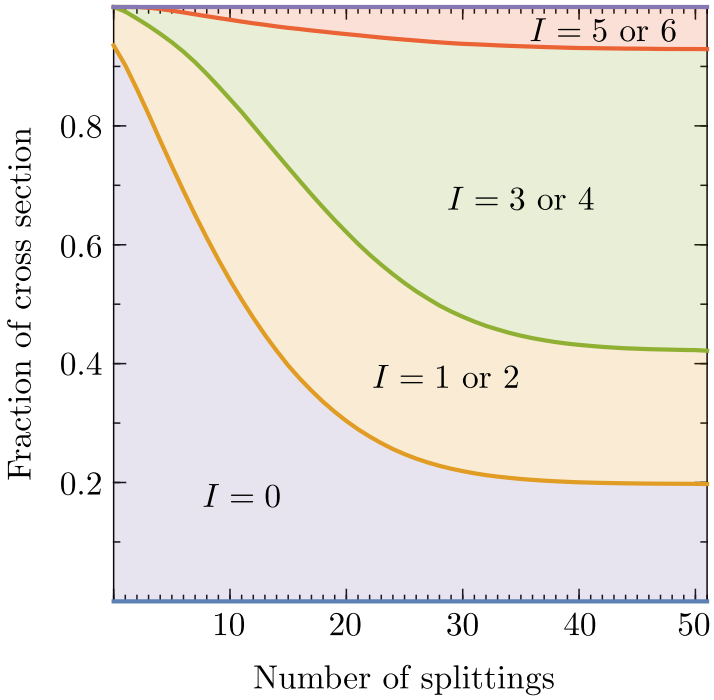

Figure 2. Fraction of events with given values, I, of the color suppression index as a function of the number of splittings. We set a limit of 4 on the change of I after the hard scattering.

4 Jet cross section

We have seen that most of the cross section to make jets in proton-proton collisions at $\sqrt{s} = 14$ TeV is associated with partonic states at the end of the parton shower that have color suppression index $I > 0$. Does this matter for the jet production cross section?

One would expect that it does not matter, since the jet production cross section is so inclusive. That is, by design, the cross section to make a jet with a certain p_{T} in a rapidity range $-2 < y < 2$ is very much infrared safe. The cross section is mostly determined by the cross section for parton-parton scattering (calculated at Born level in this case).

Parton shower evolution can add some p_{T} to the jet from partons radiated from the initial state partons. Shower evolution can also subtract some p_{T} from the jet when the scattered parton that initiates the jet radiates a gluon at such a wide angle that the gluon is not included in the jet. This initial state and final state radiation, along with the interference between initial state and final state radiation, is influenced by the color configuration of the radiating partons. Thus the development of the color configuration can influence the ultimate jet cross section. Since the color state develops differently in the LC+ approximation than it does in the LC approximation, the jet cross section could be affected. However, since the jet cross section is designed to be insensitive to all of these infrared or long-time effects, one does not expect to see much difference between the jet cross section calculated in the LC+ approximation and the jet cross section calculated in

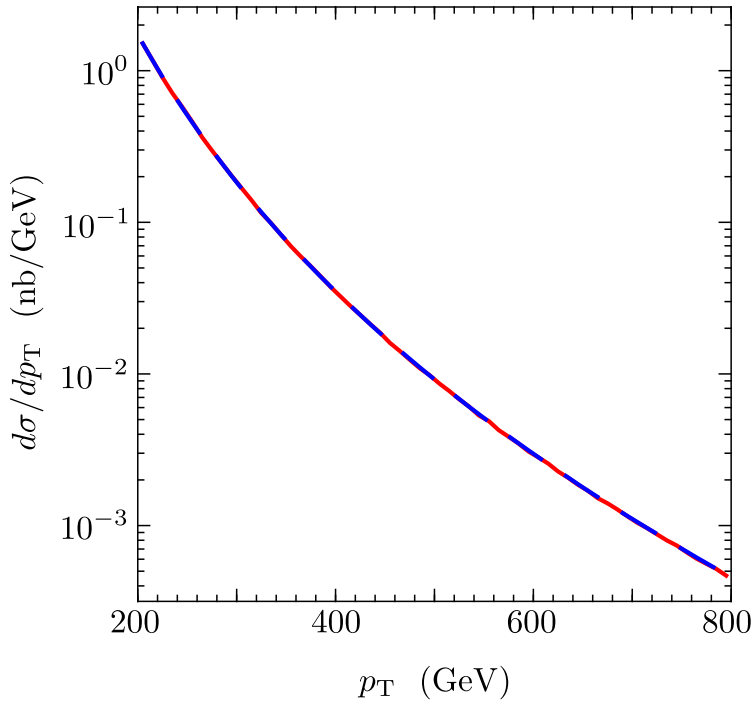

Figure 3. One jet inclusive cross section $d\sigma/dp_T$ for $|y| < 2$ using the k_T algorithm with $R = 0.4$. The red solid line shows the cross section calculated with the LC+ approximation. The blue dashed line shows the cross section calculated with the LC approximation for the parton shower. The two curves are indistinguishable.

the LC approximation.

We can test the hypothesis that the LC approximation gives a jet cross section close to that of the LC+ approximation. We use DEDUCTOR to calculate the one jet inclusive cross section $d\sigma/dp_T$ to produce a jet with transverse momentum p_T in the rapidity range $-2 < y < 2$. With the help of FASTJET [13], we use the k_T jet algorithm [14, 15] with $R = 0.4$. The results are shown in figure 3. The solid line shows the cross section calculated with the LC+ approximation with $(\Delta I)_{\max} = 4$. The dashed line shows the result obtained with the LC approximation.[3] The dashed line and the solid line are indistinguishable on the graph. We would show a graph of the ratio of the two cross sections, but we find that the difference is less than 2%, which is the statistical accuracy of the calculation.

We conclude that the use of the LC approximation for the shower instead of the LC+ approximation makes a negligible difference for the one jet inclusive cross section, even though most of the cross section comes from states that have color suppression index $I > 0$ by the end of the shower. This is not a surprising conclusion, but it is not a conclusion

[3] In the hard scattering, density matrix contributions $|\{c\}_2\rangle\langle\{c'\}_2|$ with $\{c\}_2 \neq \{c'\}_2$ are eliminated and the corresponding cross section is redistributed to density matrix contributions $|\{c\}_2\rangle\langle\{c'\}_2|$ with $\{c\}_2 = \{c'\}_2$. Then $(\Delta I)_{\max}$ is set to zero in the shower so that the color suppression index stays equal to zero.

that one could be sure of without doing the calculation.

5 Number of partons in a jet

In section 4 we looked at an observable that is very insensitive to soft parton splittings: the one jet inclusive cross section. Now, we look inside these jets at a quantity that is *sensitive* to soft parton splittings: the distribution of the number of partons in a jet. Evidently, the number of partons in a jet is not a physical observable, but it is calculable with a fixed cut on the smallest transverse momentum allowed in a parton splitting. It is a stand-in for the number of hadrons in a jet, which is physically observable. The distribution of the number of partons in a jet is of interest here because it is an infrared sensitive quantity.

We analyze a sample of jets with $p_{\mathrm{T}} > 200$ GeV and $|y| < 2$. We examine the distribution $\rho_n(n)$ of the number n of partons in a jet in this sample for events simulated by DEDUCTOR using the LC+ approximation and using the LC approximation. The distribution is normalized to $\sum_n \rho_n(n) = 1$. In each case, we stop the shower by not allowing any splittings with a splitting transverse momentum smaller than $k_{\mathrm{T}}^{\mathrm{min}} = 1$ GeV.

The result is displayed in figure 4. We see that for $n < 10$, $\rho_n(n)$ is quite insensitive to whether we use the LC or LC+ approximation. The behavior of $\rho_n(n)$ for large n is of special interest because when there are many partons, most of them must have small momenta, so that for large n we probe the softest emissions. The probability that there are more than 10 partons in a jet is small. We notice that for $n > 10$, $\rho_n(n)$ calculated using the LC+ approximation is about 10% larger than $\rho_n(n)$ calculated using the LC approximation. The fractional difference is of order $1/N_{\mathrm{c}}^2$, in accordance with the simplest expectation.

6 Gap fraction

We now turn to an observable for which we find that the color treatment matters: the probability that there are no jets in the rapidity range between two jets that are widely separated in rapidity.

In proton-proton collisions at $\sqrt{s} = 14$ TeV, we look for jets using the k_{T} algorithm with $R = 0.4$. We select events for which there is at least one jet with transverse momentum $p_{\mathrm{T}} > 200$ GeV and rapidity $y > 2$ and at least one jet with transverse momentum $p_{\mathrm{T}} > 200$ GeV and rapidity $y < -2$. Evidently this situation is most likely to arise from parton scattering with a rather small scattering angle: $\theta_{\mathrm{max}} \approx 2e^{-2} = 0.27$. The energy of each of the colliding partons is then at least 200 GeV$/\tan(\theta_{\mathrm{max}}) \approx 720$ GeV.

The probability to produce more than the required two large p_{T} jets is suppressed by a factor α_{s} and by the need to have parton distribution functions with larger momentum fraction arguments. Thus we expect that in the region $-2 < y < 2$ there will most often be a gap containing no large p_{T} jets. However, it is easily possible to produce additional smaller p_{T} jets in the gap region, $-2 < y < 2$, by initial state or final state radiation. For a given transverse momentum $p_{\mathrm{T}}^{\mathrm{cut}}$, we can ask for the fraction $f(p_{\mathrm{T}}^{\mathrm{cut}})$ of selected events in which no jet that has transverse momentum greater than $p_{\mathrm{T}}^{\mathrm{cut}}$ appears in the gap region.

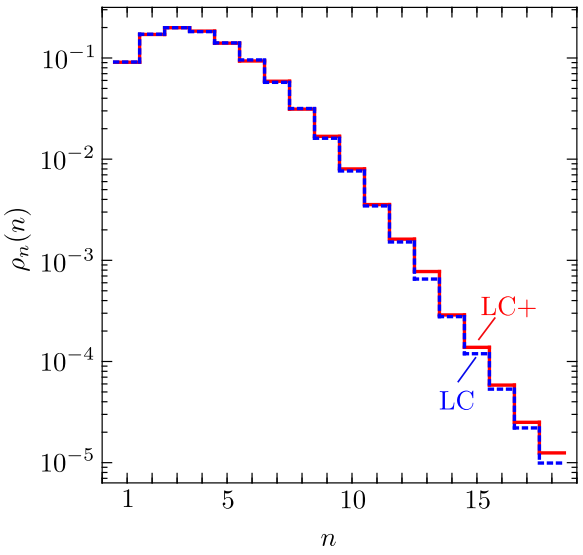

Figure 4. The distribution $\rho_n(n)$ for the number n of partons in a jet with $p_T > 200$ GeV and $|y| < 2$. We compare the distribution calculated with the LC+ approximation (solid red histogram) with the with the same distribution calculated with the LC approximation (dashed blue histogram). The results are very close for $n < 10$. The jets are constructed using the k_T algorithm with $R = 0.4$.

It is of some importance to understand the gap fraction f because it is often useful in experimental investigations to impose a requirement that there be some minimum number of high p_T jets in an event but no jets beyond this that have p_T greater than some value p_T^{cut}. In addition, the behavior of f as a function of how the gap is defined is a matter of substantial theoretical interest because it brings together several issues concerning the structure of QCD. Many of these issues are reviewed in ref. [16].

In figure 5, we plot $f(p_T^{cut})$, versus p_T^{cut}. For large values of p_T^{cut}, we expect $f(p_T^{cut})$ to be close to 1. However, it is typically rather easy to produce low transverse momentum jets, so for small p_T^{cut}, we expect $f(p_T^{cut})$ to be small. This is what we see in figure 5. We have calculated p_T^{cut} both in the LC approximation and in the LC+ approximation. We see that there is about a 10% difference between the two results at small values of p_T^{cut}. This level of difference is similar to what we saw for the distribution of the number of partons in a jet in section 5. In the remainder of this section, we will use the LC+ approximation and examine how $f(p_T^{cut})$ is affected by the color structure of the state just after the hard scattering.

The rate of decrease of $f(p_T^{cut})$ as p_T^{cut} decreases is controlled by the color flow in the event. To see this from the point of view of a dipole based parton shower, consider gluon-gluon scattering, as depicted in figure 6. Partons "a" and "b" scatter to produce final state partons 1 and 2. Parton "a" has infinite positive rapidity, while parton "b" has infinite negative rapidity. Scattering via gluon exchange, as here, has a large probability to be small angle scattering, so this diagram is a leading diagram for the case of interest, in which parton 1 has large positive rapidity and parton 2 has large negative rapidity. In a

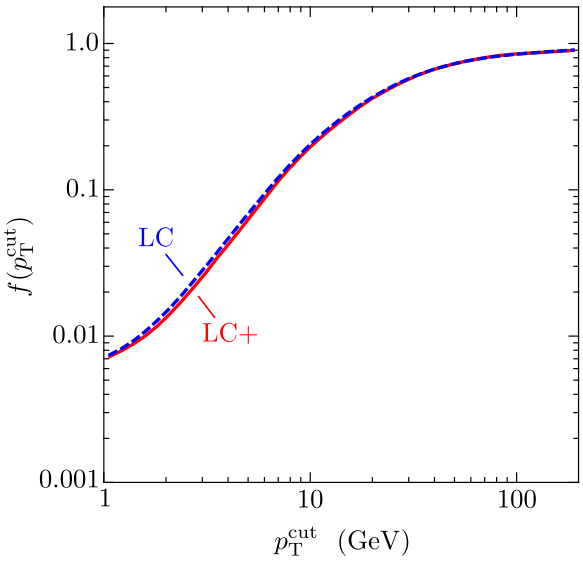

Figure 5. For events with at least one jet with transverse momentum $p_T > 200$ GeV and rapidity $y > 2$ and at least one jet with transverse momentum $p_T > 200$ GeV and rapidity $y < -2$, we plot the fraction $f(p_T^{cut})$ of events that have no jets with transverse momentum greater than p_T^{cut} in the rapidity range $-2 < y < 2$. The blue dashed curve shows the result obtained with the LC approximation and the red solid curve shows the result obtained with the LC+ approximation.

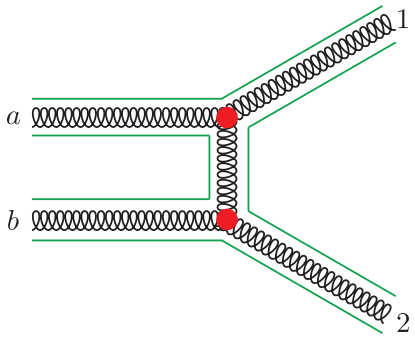

Figure 6. Gluon-gluon scattering via gluon exchange

leading color picture, partons "a" and "b" are color connected, as are "a" and 1, "b" and 2, and 1 and 2, as indicated in figure 6. There is another color configuration in which "a" is connected to 2 and "b" is connected to 1.

These parton pairs form color dipoles. In a parton shower, the a-1 pair produces soft radiation in the angular region between $\vec{p}_a$ and $\vec{p}_1$. That is, this radiation has large positive rapidity. Similarly, the b-2 dipole produces soft radiation with large negative rapidity. The a-b dipole produces soft radiation with any rapidity between a large positive value and a large negative value. Similarly, the 1-2 dipole produces soft radiation with any rapidity between the large positive rapidity of parton 1 and a large negative rapidity of parton 2.

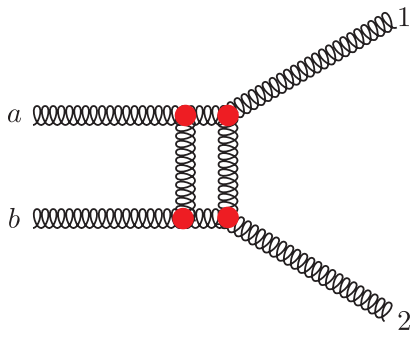

Figure 7. A virtual correction to gluon-gluon scattering

Thus it is very likely that the a-b, 1-2, a-2, and b-1 dipoles will produce radiation that fills in the gap.

Now consider the effect of a correction to the graph of figure 6 from the exchange of a virtual gluon between partons "a" and "b," as illustrated in figure 7. The exchange of two gluons is equivalent in color space to the exchange of an object with color **27**, color **10**, color $\overline{\mathbf{10}}$, color **8** (in two ways), or color **1**. With color singlet exchange, the two forward moving partons, "a" and 1, are completely disconnected in color space from the two backward moving partons, "b" and 2. Soft gluon radiation from this color configuration gives forward radiation and backward radiation, but only a small amount of radiation into the gap region. Thus when the parton shower starts from this configuration, the gap fraction $f(p_{\mathrm{T}}^{\mathrm{cut}})$ can remain not-too-small for small $p_{\mathrm{T}}^{\mathrm{cut}}$.

This same argument applies to virtual gluon exchange between partons 1 and 2. It also applies to virtual gluon exchange between "a" and 2 or between "b" and 1. It also applies to q-g scattering, q-q scattering, and q-$\bar{q}$ scattering.

We conclude that to investigate the probability $f(p_{\mathrm{T}}^{\mathrm{cut}})$ for gap preservation, we should include the effects of virtual gluon exchange. Here, we need to note some features of the color treatment in DEDUCTOR. First, in a parton shower like DEDUCTOR, an approximation to the effects of virtual parton exchange is contained in the Sudakov factor that appears between one real splitting and the next. Second, DEDUCTOR uses a certain (and rather standard [12]) basis for the partonic color space for an arbitrary number of partons [4, 8]. The splitting operator and the Sudakov exponent for the shower are matrices defined using this basis. Unfortunately, we do not know how to use these matrices exactly, so DEDUCTOR uses approximate versions defined by the LC+ approximation.

The virtual gluon exchange amplitude has an imaginary part, proportional to $\mathrm{i}\pi$, when the exchange is between two final state partons or between the two initial state partons. This part is not normally included in the Sudakov exponent, and is not included in DEDUCTOR. However, it can be included to the extent that it is consistent with the LC+ approximation [8]. Unfortunately, even if we include the $\mathrm{i}\pi$, the effect that we are looking for is dropped in the LC+ approximation. This is because, in the effect that we need to include, the operator in the Sudakov exponent changes the parton color description from

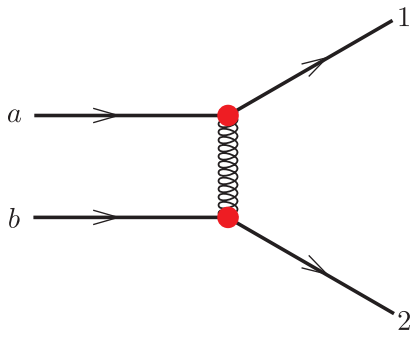

Figure 8. Quark-quark scattering via gluon exchange

one color basis state to another, while the LC+ approximation is designed to omit all such color changing contributions [8]. As explained in ref. [8], it is possible (at least in principle) to include these effects perturbatively. However, this perturbative treatment is not yet implemented in DEDUCTOR.

We have seen that the color changing effect of virtual gluon exchange can be physically important, but that we do not model this effect properly with the current version of DEDUCTOR. We can, however, study a very similar effect numerically. The effect emerges not because a parton shower using the LC+ approximation is nearly perfect but because it is imperfect. It happens that within this approximation an effect emerges that is similar to the effect that should occur in a better color approximation: the system can get to a color state in which there is very little radiation into the gap.

We see this effect by looking at quark-quark scattering as illustrated in figure 8. The hard scattering amplitude with which the shower starts is a linear combination of two of DEDUCTOR's standard color basis vectors, which are illustrated in figure 9. In state $\big|\text{conn}\big\rangle$, quark "a" with positive rapidity is color connected to quark 2 with negative rapidity, while quark "b" with negative rapidity is color connected to quark 1 with positive rapidity. That is, the color connections span the rapidity range of the gap region. This contrasts with $\big|\text{disc}\big\rangle$, in which the partons with positive rapidity are disconnected in color space from the partons with negative rapidity.

The color density matrix that arises from figure 8 thus has the form

$$\rho = \big|\text{conn}\big\rangle\rho_{\text{cc}}\big\langle\text{conn}\big| + \big|\text{conn}\big\rangle\rho_{\text{cd}}\big\langle\text{disc}\big| + \big|\text{disc}\big\rangle\rho_{\text{dc}}\big\langle\text{conn}\big| + \big|\text{disc}\big\rangle\rho_{\text{dd}}\big\langle\text{disc}\big| \ . \tag{6.1}$$

We can divide this into two terms. The first is

$$\rho(\text{conn}) = \big|\text{conn}\big\rangle\rho_{\text{cc}}\big\langle\text{conn}\big| + \big|\text{conn}\big\rangle\rho_{\text{cd}}\big\langle\text{disc}\big| + \big|\text{disc}\big\rangle\rho_{\text{dc}}\big\langle\text{conn}\big| \ , \tag{6.2}$$

which we call the connected contribution. The second is

$$\rho(\text{disc}) = \big|\text{disc}\big\rangle\rho_{\text{dd}}\big\langle\text{disc}\big| \ , \tag{6.3}$$

which we call the disconnected contribution.

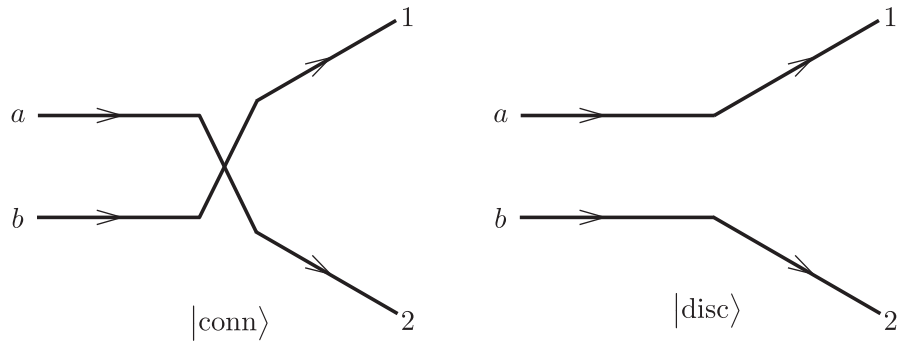

Figure 9. Two color states contributing to quark-quark scattering.

The definition of the connected and disconnected contributions to the color density matrix can be generalized to gluons as well as quarks and to more partons. We assume that some of the partons are moving to the right, with large positive rapidities and some are moving to the left, with large negative rapidities. In the color basis [4, 8] that we use, each quark or antiquark in the ket state has one color connected partner and each gluon has two. The same applies to the bra state. If, in both the bra and ket states, the color connected partners of each right moving parton are also right moving partons and the color connected partners of each left moving parton are also left moving partons, then the corresponding contribution to the color density matrix is "disconnected." Otherwise, it is connected.

For q-$\bar{q}$ scattering and $\bar{q}$-$\bar{q}$ scattering as well as q-q scattering, there are both connected and disconnected contributions just after the hard scattering. The disconnected contributions come with factors proportional to $1/N_c^2$. For q-g scattering, $\bar{q}$-g scattering, and g-g scattering, all of the contributions are in the connected class.

It is rather uncertain what nomenclature one should use for $\rho(\text{disc})$. The coefficient ρ_{dd} in $\rho(\text{disc})$ contains a factor $1/N_c^2$. Thus $\rho(\text{disc})$ is a color suppressed contribution to the cross section. Arguably, one should leave it out of the leading color approximation. However, the bra and ket color states in $\rho(\text{disc})$ are the same, so, arguably, one should include it in the leading color approximation. In DEDUCTOR at the beginning of the shower, we set the color suppression index for this contribution to zero and we include it in the DEDUCTOR leading color option.

We expect that for contributions for which the shower starts from from $\rho(\text{conn})$, soft radiation into the gap region will be likely. Thus the gap fraction $f(p_T^{\text{cut}})$ should be small for small p_T^{cut}. We also expect that for contributions for which the shower starts from $\rho(\text{disc})$, soft radiation into the gap region will be unlikely, so that $f(p_T^{\text{cut}})$ for this part of the cross section should be not very small for small p_T^{cut}. These expectations are verified by a calculation in DEDUCTOR displayed in figure 10. For these results, we used the LC+ approximation.

The total gap fraction, $f(p_T^{\text{cut}})$, from figure 5 is also shown in figure 10. The total gap fraction is an average of the connected and disconnected contributions, weighted by their

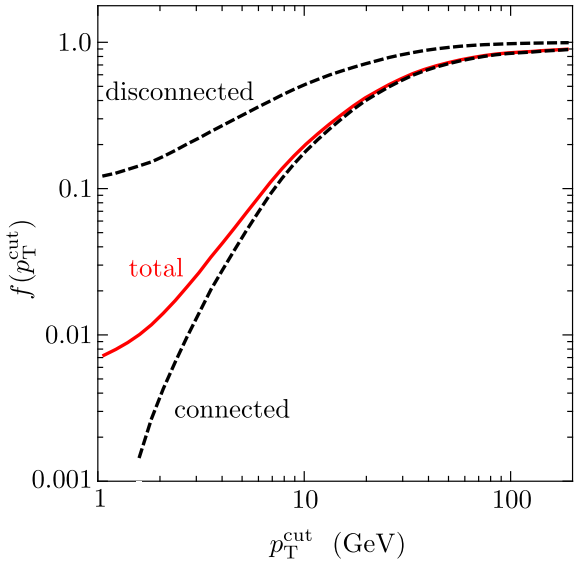

Figure 10. Fraction $f(p_T^{cut})$ of events in which no jets with transverse momentum greater than p_T^{cut} appear in the gap region, as in figure 5. The red solid curve shows the result obtained with the LC+ approximation, as in figure 5. The upper black dashed curve shows $f(p_T^{cut})$ corresponding to events in which the starting color state has the property that the right moving partons are color disconnected from the left moving partons. That is, no color-connected partner of a right-moving parton is a left moving parton, either in the ket state or the bra state. The lower black dashed curve shows $f(p_T^{cut})$ corresponding to events that are not color disconnected in this sense.

respective cross sections, which are in a ratio of about 15 to 1. Because the cross section for the disconnected contribution is so small, this contribution is not so important for large values of p_T^{cut}. However, it becomes relatively more important as p_T^{cut} decreases.

There is quite a lot of complexity in the structure of QCD as it affects the gap fraction f. At a first level in an analytic summation of leading logarithms [17, 18], one uses the exponential of a Sudakov exponent constructed from one loop graphs for the virtual exchange of a low transverse momentum gluon. This includes the imaginary parts proportional to $i\pi$. The Sudakov exponent is a matrix in the color space for two incoming partons and two outgoing partons. The full matrix is exponentiated, with no approximation similar to the LC+ approximation. One finds that the starting color state produced by the hard parton-parton scattering has a non-zero projection onto an eigenvector of the Sudakov exponent that corresponds to very little virtual emission into the gap and accordingly a gap fraction f that is not very small. This is qualitatively similar to what we see in figure 10, but the result in figure 10 cannot be quantitatively correct compared to this level of analytic summation of leading logarithms because the parts of the Sudakov exponent that are dropped in the LC+ approximation are important to the full color result.

There are further subtleties in the analytic treatment. When the rapidity separation Δy between the leading jets is large, factors of Δy in the exponent are especially important [19]. There can also be real emissions of gluons outside the gap. These gluons can create

virtual emission of low transverse momentum gluons into the gap. This creates "non-global" logarithms with a different structure than seen in the simplest analytic treatment [20–23]. Furthermore, some of these logarithms are "super-leading" in the sense of having more powers of logarithms per power of α_s than one gets in the simple analysis [16, 24–26]. For the purpose of capturing these effects, there is an advantage to using a parton shower approach, which can trace the emission of real gluons outside the gap and the subsequent virtual radiation from these gluons. However, a better treatment of color within the shower is needed to realize this advantage.

7 Comparison to experiment for the gap fraction

It is of interest to compare DEDUCTOR results to experimental results from Atlas for the gap fraction [27], even though we understand that the color treatment in DEDUCTOR is incomplete. In the Atlas results, p_T^{cut} is fixed and the gap fraction f is plotted as a function of the transverse momentum of the hard jets. This contrasts with fixing the hard jet transverse momenta to be bigger than 200 GeV and plotting f versus p_T^{cut}, as in figures 5 and 10. Specifically, Atlas uses a data sample at $\sqrt{s} = 7$ TeV. Jets are defined using the anti-k_T algorithm [28] with $R = 0.6$. All jets in the rapidity window $-4.4 < y < 4.4$ are considered if they have $p_T > p_T^{cut} = 20$ GeV. Of these jets, the two jets with the highest p_T are selected. Of the two leading jets, let jet 1 have the highest rapidity and let jet 2 have the lowest rapidity. The event is characterized by the rapidity difference $\Delta y = y_1 - y_2$ and the average transverse momentum $\bar{p}_T = (p_{T,1} + p_{T,2})/2$. The event has a gap if there is no jet (with $p_T > p_T^{cut}$) in the rapidity range $y_1 < y < y_2$. Only a fraction f of events with a given Δy and $\bar{p}_T$ has a gap.

In figure 11, we exhibit the Atlas results for the gap fraction f as a function of $\bar{p}_T$ for events with Δy in five different ranges. We compare these to the corresponding predictions from DEDUCTOR. We note that the DEDUCTOR gap fraction is generally too large. That is, DEDUCTOR is producing too little soft radiation in the gap region. Now, DEDUCTOR lacks an underlying event. One would expect that radiation from an underlying event would increase the probability for a jet to appear in the gap region and would thus decrease the gap fraction. Additionally, if a hadronization model were included in DEDUCTOR, there would likely be some change in the results. At larger values of Δy, the discrepancies are larger. This is presumably an indication that the LC+ approximation is missing important physics related to representing factors in the Sudakov exponent proportional to Δy. Notice that for the larger values of Δy, the DEDUCTOR curves decrease very slowly as $\bar{p}_T$ increases. In fact, for $5 < \Delta y < 6$, the DEDUCTOR curve even increases as $\bar{p}_T$ increases for large $\bar{p}_T$. This can be at least partly attributed to a kinematic effect: for large $\bar{p}_T$ and Δy, it is difficult to find partons in the protons with enough energy to make more jets. Qualitatively, this effect seems to be present in the data. For the largest values of $\bar{p}_T$ and Δy, there are no events in the data sample.

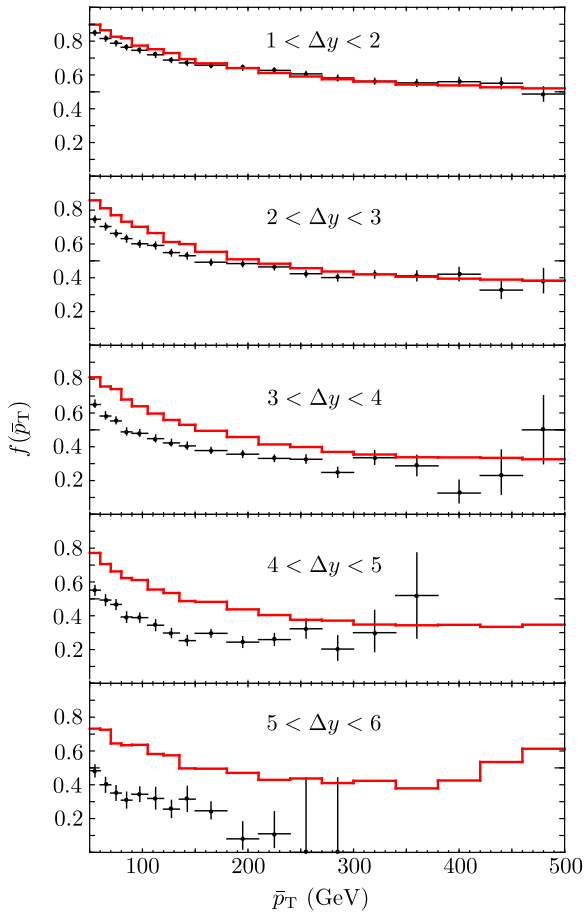

Figure 11. Fraction $f(\bar{p}_T)$ of events in which no jets with transverse momentum greater than $p_T^{cut} = 20$ GeV appear in the gap region. There are five plots, corresponding to five ranges for the rapidity separation between the leading jets. The leading jets have an average transverse momentum $\bar{p}_T$. The red solid curves show the result obtained with the LC+ approximation, as in figure 5. The black points with error bars are data from Atlas [27].

8 Conclusions and outlook

We have examined the effect of color flow on the results from a parton shower generator based on color dipoles, DEDUCTOR. On one hand, we used the leading color, LC, approximation that is standard for parton shower generators. We compared LC results to results from the LC+ approximation that is available in DEDUCTOR. We used the LC+ approximation up to terms suppressed by more than four powers of $1/N_c$. The LC+ approximation has the advantage that it is exact in color for collinear emissions. It is, however, only approximate for wide angle soft gluon emissions.

By comparing LC results to LC+ results, we tested numerically how good the LC approximation is. We found that the LC approximation is quite good for the one jet inclusive cross section and for the distribution of the number of partons in a jet. There is an important caution needed here: one would really need to test the LC approximation

against a full color treatment to be sure that the LC approximation is accurate for any given observable. However, testing the LC approximation against the LC+ approximation certainly gives the LC approximation a chance to fail and it does not.

We have reported results for only two simple observables, but we have tried some other observables and have found similar results.

In section 3, we asked how much color suppression is typical. We found that color evolution beyond the leading color approximation is not rare. It is the norm. However, we find that simple observables are not much affected by deviations from leading color configurations.

In one case, we found that the LC approximation is not adequate: the gap-between-jets cross section investigated in sections 6 and 7. Here the LC+ approximation is also inadequate. We know this on theoretical grounds: the color changing operators that need to be present are in fact not present in the LC+ approximation. We also saw in figure 10 that there is a substantial numerical difference in the gap fraction f between color states that are likely (with our approximations) to radiate into the gap and color states that are unlikely to radiate into the gap. Furthermore, we saw a breakdown of the LC+ theory compared to experiment in section 7.

We believe that a parton shower approach to the gap-between-jets problem holds some promise because a parton shower approach can sometimes provide numerical results to complicated problems that are too unwieldy to solve analytically. For instance, a parton shower automatically includes potential radiation into the gap from a gluon that was radiated out of the gap. What is needed is a better treatment of color within the parton shower. In ref. [8], we described how one can insert perturbatively the evolution operators that represent the difference between exact color and the LC+ approximation. It is perhaps not necessary to have a large number of insertions in order to have a reasonably good approximation: one virtual gluon exchange in the ket state and one in the bra state may be enough. We have not, however, implemented such a program, so we do not know how well it will work.

Our tests do not include hadronization. We anticipate in the future linking Deductor to the string hadronization model [29, 30] of Pythia. For this purpose, we need to specify the probability for a given color density matrix element $\big|\{c\}_m\big\rangle\big\langle\{c'\}_m\big|$ from eq. (2.1) to correspond to a given classical string state. A method for doing this is given in section 8 of ref. [8]. We expect that the string configurations produced with the LC+ approximation may have more kinks than those produced with the LC approximation. Presumably this will necessitate retuning the parameters of the hadronization model compared to the Pythia default tune. It is difficult to predict what effects may remain after retuning.

Acknowledgments

This work was supported in part by the United States Department of Energy and by the Helmholtz Alliance "Physics at the Terascale." We thank Jeff Forshaw and Mrinal Dasgupta for helpful conversations about rapidity gap physics. We thank Stephanie Majewski for advice about statistical conventions in data analysis.

A Using the leading color approximation

DEDUCTOR uses the LC+ approximation for color, as explained in some detail in ref. [8]. However, we may want to use just an LC shower. In particular, it is useful to turn the LC+ shower off if the amount that the color suppression index has increased during the shower (after the hard interaction) reaches a preset value, $(\Delta I)_{\max}$. After that, we can proceed with an LC shower. The leading color approximation is commonly used in parton shower algorithms, so it would hardly need an explanation. However, we need to run an LC shower starting with a color density matrix

$$\rho(\{p,f\}_m,t) = \sum_{\{c\}_m,\{c'\}_m} \rho(\{p,f,c',c\}_m,t)\,\big|\{c\}_m\big\rangle\big\langle\{c'\}_m\big|\,, \tag{A.1}$$

where possibly $\{c'\}_m \neq \{c\}_m$. This is straightforward, but it is not commonly done, so we explain it in this appendix. In order to keep the appendix brief, we assume that the material in refs. [4] and [8] is known.

The method for switching from LC+ to LC that we explain here and that is implemented in DEDUCTOR is different from the method outlined in appendix C of ref. [8].

The LC approximation is based on replacing the color group $SU(N_c)$ by $U(N_c)$. There are N_c^2 gluons, labeled with $q = \{1,2,\ldots,N_c^2\}$. The generator matrices $t^1,\ldots,t^{N_c^2-1}$ in the fundamental representation are the usual ones. The new generator is

$$t^{N_c^2}_{ii'} = \frac{1}{\sqrt{2N_c}}\,\delta_{ii'}\,. \tag{A.2}$$

This gives the identity

$$\sum_{a=1}^{N_c^2} t^a_{ii'}t^a_{jj'} = \frac{1}{2}\,\delta_{ij'}\delta_{ji'}\,. \tag{A.3}$$

That is, aside from the factor 1/2, we can think of each gluon as carrying one color N_c line and one color $\bar{N}_c$ line. The factor $T_R = 1/2$ comes from our conventional normalization of the generator matrices,

$$\mathrm{Tr}[t^a t^b] = \frac{1}{2}\,\delta_{ab}\,. \tag{A.4}$$

With the definition Eq. (A.2), this normalization remains true for all a and b.

We define the structure constants f_{abc} that give the couplings of the gluons to each other by

$$[t^a,t^b] = \mathrm{i} f_{abc} t^c\,. \tag{A.5}$$

With this definition, we see that the $U(1)$ gluon that we have added, with index N_c^2, does not couple to the other gluons. That is, $f_{abc} = 0$ if any of a, b, or c is N_c^2.

Our analysis makes use of the standard color basis defined by two sorts of vectors, as in ref. [4]. First, there are open string vectors

$$\Psi(S)^{\{a\}} = N(S)^{-1/2}[t^{a_2}t^{a_3}\cdots t^{a_{n-1}}]_{a_1,a_n}\,. \tag{A.6}$$

Here a_1 is a quark color index, a_n is an antiquark color index, and the other a_i are gluon color indices. The t^a are $U(N_c)$ color matrices in the fundamental representation. Also,

$N(S) = N_c(N_c/2)^{n-2}$ is a normalization factor such that $\langle\Psi|\Psi\rangle = 1$. Second, there are closed string vectors

$$\Psi(0)^{\{a\}} = N(S)^{-1/2}\,\mathrm{Tr}[t^{a_1}t^{a_2}\cdots t^{a_n}] \ . \tag{A.7}$$

Here all of the a_i are gluon color indices. Again, $N(S) = (N_c/2)^n$ is a normalization factor such that $\langle\Psi|\Psi\rangle = 1$. (With $SU(N_c)$, $\langle\Psi|\Psi\rangle$ is slightly different from 1.) The most general color basis vector, which we denote by $|\{c\}_m\rangle$, is a product of these two kinds of units.

The color basis states are normalized to $\langle\{c\}_m|\{c\}_m\rangle = 1$. They are not, however, generally orthogonal. However, when $\{c\}_m$ and $\{c'\}_m$ are different, one finds that $\langle\{c'\}_m|\{c\}_m\rangle = \mathcal{O}(1/N_c^2)$ or $\mathcal{O}(1/N_c)$. That is, the basis vectors are orthogonal only in the $N_c \to \infty$ limit.

The evolution equation for the shower state as a function of the shower time t has the form of a linear equation

$$\frac{d}{dt}|\rho(t)\rangle = [\mathcal{H}_I(t) - \mathcal{V}(t)]|\rho(t)\rangle \ . \tag{A.8}$$

Here $\mathcal{H}_I(t)$ is the parton splitting operator. It is given for full color in eq. (5.7) of ref. [8]. The LC+ approximation is defined in ref. [8] by restricting the possibilities for color states that can be reached by a splitting. We can define the LC approximation by restricting these choices further. This is illustrated in figures 12 and 13.

In figure 12 we illustrate the color structure for the splitting of a gluon into two gluons, numbered 1 and 3. The same splitting occurs in both the bra and ket states. Note that in this example, the color structures of the bra and ket states are not the same. Triple gluon vertices are $\mathrm{i}f_{abc}$. Using eq. (A.5), we can expand the left hand side of figure 12 into a linear combination of four products of color basis functions, as shown in the right hand side of figure 12. In the LC+ approximation, we keep all four of these terms. We define the LC approximation to keep just the first two terms. In the shower Monte Carlo algorithm, we choose one state or the other with probability 1/2.

In figure 13 we illustrate the color structure for the radiation of a gluon 3 from gluon 1 in the ket state, but with interference with the radiation of gluon 3 from "helper gluon" 2 in the bra state. Expanding the left hand side into products of basis functions produces four terms. Of these, the LC+ approximation keeps the two terms shown in the right hand side of figure 13. We define the LC approximation to keep only the first term.

The general principle for emission of a gluon should be clear from these two examples: the new gluon (3) must not cross the emitting gluon (1) in the color diagram. For emission of a gluon from a quark, the situation is simpler: there is only one allowed structure in the LC+ approximation (as in figure 16 of ref. [8]) and this structure is retained in the LC approximation. There is also the possibility of $\mathrm{g} \to q + \bar{q}$ splittings. With the color group $U(N_c)$, there is only one possible new color state after the splitting. The new state is given by connecting the new quark and antiquark to the previous color string by using eq. (A.3).

We also need the operator $\mathcal{V}(t)$ in eq. (A.8). This operator leaves the number of partons unchanged. Its exponential is the Sudakov factor that appears between splittings in the shower. We define $\mathcal{V}(t)$ from $\mathcal{H}_I(t)$ in such a way that the inclusive cross section that we started with at the hard interaction is not changed at all by the shower. The operator

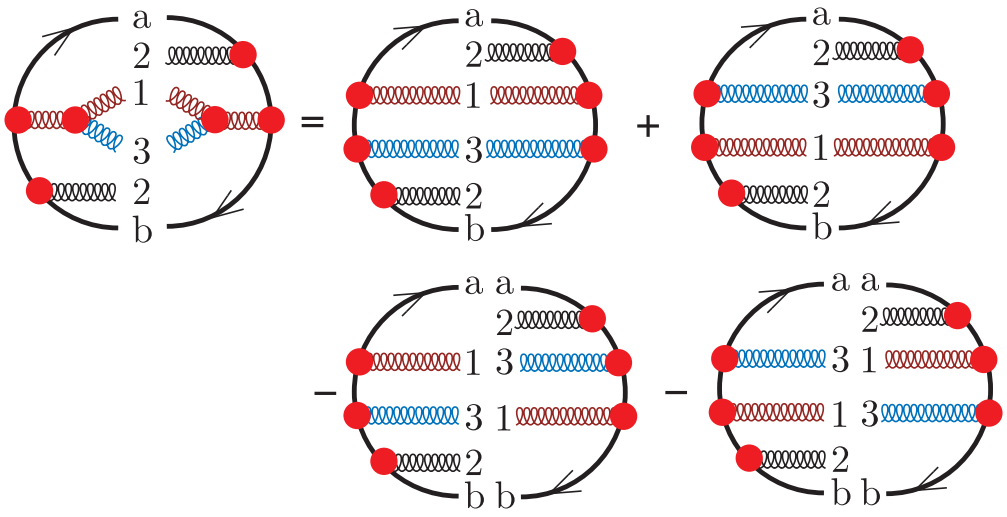

Figure 12. Identity for color dependence of splitting of gluon 1 in both the bra state and the ket state in the case $\{c'\}_m \neq \{c\}_m$. In the LC+ approximation, one keeps all four terms. In the LC approximation, we keep only the first two terms.

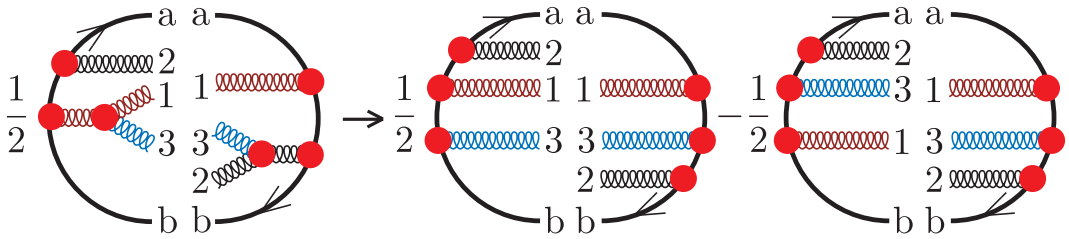

Figure 13. LC+ approximation for the splitting of gluon 1 in the ket state with the participation of helper parton 2 in the bra state in a case with $\{c'\}_m \neq \{c\}_m$. In the LC approximation, we keep only the first term.

$\mathcal{V}(t)$ contains a color factor denoted by $N(k, l, \{\hat{f}\}_{m+1})$ in ref. [8]. For the LC+ approximation, it is given in eq. (6.12) of ref. [8]. For the LC approximation, we need to calculate $N(k, l, \{\hat{f}\}_{m+1})$ using the color group $U(N_c)$ and including only the LC contributions. For all cases of gluon emission except for a $g \to g + g$ splitting as in figure 12, $N(k, l, \{\hat{f}\}_{m+1})$ is $N_c/2$, where the N_c comes from having one more "quark" loop and the $1/2$ is the $1/2$ in eq. (A.3). For a $g \to g + g$ splitting, there are two terms, so the net color factor in $\mathcal{V}(t)$ is $2(N_c/2) = N_c = C_A$. For a $g \to q + \bar{q}$ splitting, $N(k, l, \{\hat{f}\}_{m+1})$ is just $T_R = 1/2$.

For the case of a $q \to q + g$ splitting in either the ket state or the bra state or both, the color factor in $\mathcal{V}(t)$ is $N_c/2$ when we calculate this way. One normally uses C_F instead. We arrange to obtain the conventional net factor of C_F instead of $N_c/2$ by simply multiplying the splitting probability by $2C_F/N_c$ in $\mathcal{H}_I(t)$ for the LC approximation.

We need one more adjustment. When the change in color suppression index during the shower reaches $(\Delta I)_{\max}$, we switch from the LC+ approximation to the LC approximation

as described above. This means changing the rules for calculating the color factor in quantum probabilities. If the color state before this switch is $\big|\{c\}_m\big\rangle\big\langle\{c'\}_m\big|$ then the corresponding contribution to the inclusive cross section contains the color factor $\big\langle\{c'\}_m\big|\{c\}_m\big\rangle_{SU(N_c)}$, where the subscript indicates a calculation using the color group $SU(N_c)$. After the switch, we have the same nominal color state, $\big|\{c\}_m\big\rangle\big\langle\{c'\}_m\big|$, but we have changed the definitions so that now the inclusive cross section contains the color factor $\big\langle\{c'\}_m\big|\{c\}_m\big\rangle_{U(N_c)}$ calculated using the color group $U(N_c)$. To preserve probabilities, we multiply the weight for the current shower state by

$$C_0 = \frac{\big\langle\{c'\}_m\big|\{c\}_m\big\rangle_{SU(N_c)}}{\big\langle\{c'\}_m\big|\{c\}_m\big\rangle_{U(N_c)}} \,. \tag{A.9}$$

This factor is normally close to 1, but in some situations the numerator can be zero. We note that DEDUCTOR contains fast algorithms for calculating both the numerator and the denominator.

References

[1] T. Sjostrand, S. Mrenna and P. Z. Skands, *A Brief Introduction to PYTHIA 8.1*, Comput. Phys. Commun. **178** (2008) 852 [arXiv:0710.3820] [INSPIRE].

[2] M. Bahr, S. Gieseke, M. A. Gigg, D. Grellscheid, K. Hamilton, O. Latunde-Dada, S. Platzer and P. Richardson *et al.*, *Herwig++ Physics and Manual*, Eur. Phys. J. C **58** (2008) 639 [arXiv:0803.0883] [INSPIRE].

[3] T. Gleisberg, S. Hoeche, F. Krauss, M. Schonherr, S. Schumann, F. Siegert and J. Winter, *Event generation with SHERPA 1.1*, JHEP **0902** (2009) 007 [arXiv:0811.4622] [INSPIRE].

[4] Z. Nagy and D. E. Soper, *Parton showers with quantum interference*, JHEP **0709** (2007) 114 [arXiv:0706.0017]] [INSPIRE].

[5] Z. Nagy and D. E. Soper, *Parton showers with quantum interference: leading color, spin averaged*, JHEP **0803** (2008) 030 [arXiv:0801.1917] [INSPIRE].

[6] Z. Nagy and D. E. Soper, *A parton shower based on factorization of the quantum density matrix*, JHEP **1406** (2014) 097 [arXiv:1401.6364] [INSPIRE].

[7] Version 1.0.2 of the code, used in this paper, is available at http://www.desy.de/∼znagy/deductor/ and http://pages.uoregon.edu/soper/deductor/.

[8] Z. Nagy and D. E. Soper, *Parton shower evolution with subleading color*, JHEP **1206** (2012) 044 [arXiv:1202.4496] [INSPIRE].

[9] Z. Nagy and D. E. Soper, *Parton showers with quantum interference: leading color, with spin*, [arXiv:0805.0216] [INSPIRE].

[10] Z. Nagy and D. E. Soper, *Ordering variable for parton showers*, JHEP **1406** (2014) 178 [arXiv:1401.6366] [INSPIRE].

[11] Z. Nagy and D. E. Soper, *Parton distribution functions in the context of parton showers*, JHEP **1406** (2014) 179 [arXiv:1401.6368] [INSPIRE].

[12] M. L. Mangano, *The Color Structure of Gluon Emission*, Nucl. Phys. B **309** (1988) 461 [INSPIRE].

[13] M. Cacciari, G. P. Salam and G. Soyez, *FastJet User Manual*, Eur. Phys. J. C **72** (2012) 1896 [arXiv:1111.6097] [INSPIRE].

[14] S. Catani, Y. L. Dokshitzer, M. H. Seymour, and B. R. Webber, *Longitudinally invariant K_t clustering algorithms for hadron hadron collisions*, Nucl. Phys. B **406** (1993) 187 [inSPIRE].

[15] S. D. Ellis and D. E. Soper, *Successive combination jet algorithm for hadron collisions*, Phys. Rev. D **48** (1993) 3160 [hep-ph/9305266] [inSPIRE].

[16] J. Forshaw, J. Keates and S. Marzani, *Jet vetoing at the LHC*, JHEP **0907** (2009) 023 [arXiv:0905.1350] [INSPIRE].

[17] N. Kidonakis, G. Oderda and G. F. Sterman, *Evolution of color exchange in QCD hard scattering*, Nucl. Phys. B **531** (1998) 365 [hep-ph/9803241] [INSPIRE].

[18] G. Oderda and G. F. Sterman, *Energy and color flow in dijet rapidity gaps*, Phys. Rev. Lett. **81** (1998) 3591 [hep-ph/9806530] [INSPIRE].

[19] J. R. Forshaw, A. Kyrieleis and M. H. Seymour, *Gaps between jets in the high energy limit*, JHEP **0506** (2005) 034 [hep-ph/0502086] [INSPIRE].

[20] M. Dasgupta and G. P. Salam, *Resummation of nonglobal QCD observables*, Phys. Lett. B **512** (2001) 323 [hep-ph/0104277] [INSPIRE].

[21] C. F. Berger, T. Kucs and G. F. Sterman, *Energy flow in interjet radiation*, Phys. Rev. D **65** (2002) 094031 [hep-ph/0110004] [INSPIRE].

[22] M. Dasgupta and G. P. Salam, *Accounting for coherence in interjet E(t) flow: A Case study*, JHEP **0203** (2002) 017 [hep-ph/0203009] [INSPIRE].

[23] R. B. Appleby and M. H. Seymour, *Nonglobal logarithms in interjet energy flow with kt clustering requirement*, JHEP **0212** (2002) 063 [hep-ph/0211426] [INSPIRE].

[24] J. R. Forshaw, A. Kyrieleis and M. H. Seymour, *Super-leading logarithms in non-global observables in QCD*, JHEP **0608** (2006) 059 [hep-ph/0604094] [INSPIRE].

[25] J. R. Forshaw, A. Kyrieleis and M. H. Seymour, *Super-leading logarithms in non-global observables in QCD: Colour basis independent calculation*, JHEP **0809** (2008) 128 [arXiv:0808.1269] [INSPIRE].

[26] R. M. Duran Delgado, J. R. Forshaw, S. Marzani and M. H. Seymour, *The dijet cross section with a jet veto* JHEP **1108** (2011) 157 [arXiv:1107.2084] [INSPIRE].

[27] G. Aad *et al.* [ATLAS Collaboration], *Measurement of dijet production with a veto on additional central jet activity in pp collisions at $\sqrt{s} = 7$ TeV using the ATLAS detector*, JHEP **1109** (2011) 053 [arXiv:1107.1641] [INSPIRE].

[28] M. Cacciari, G. P. Salam and G. Soyez, *The Anti-k(t) jet clustering algorithm*, JHEP **0804** (2008) 063 [arXiv:0802.1189] [INSPIRE].

[29] B. Andersson, G. Gustafson, G. Ingelman and T. Sjostrand, *Parton Fragmentation and String Dynamics*, Phys. Rept. **97** (1983) 31 [INSPIRE].

[30] T. Sjostrand, *Jet Fragmentation of Nearby Partons*, Nucl. Phys. B **248** (1984) 469 [INSPIRE].